Optics Communications 305 (2013) 236–239

Contents lists available at SciVerse ScienceDirect

Optics Communications

journal homepage: www.elsevier.com/locate/optcom

Response time improvement of liquid–crystal wavefront corrector using optimal cell gap of numerical computation

Qidong Wang [a,b], Zenghui Peng [a,*], Qianqian Fang [a,b], Xiaoping Li [a,b], Mengjiao Qi [a,b], Yonggang Liu [a], Lishuang Yao [a], Zhaoliang Cao [a], Quanquan Mu [a], Li Xuan [a]

[a] State Key Laboratory of Applied Optics, Changchun Institute of Optics, Fine Mechanics and Physics, Chinese Academy of Sciences, Changchun 130033, PR China

[b] Graduate School of Chinese Academy of Sciences, Beijing, 100039, PR China

ARTICLE INFO

Article history:
Received 22 March 2013
Received in revised form
6 May 2013
Accepted 7 May 2013
Available online 28 May 2013

Keywords:
Liquid crystal
Wavefront corrector
Response time
Finite differences

ABSTRACT

The optimal cell gap of nematic liquid–crystal wavefront corrector (LCWFC) is proved theoretically by numerical computation of the Ericksen–Leslie equation based on finite differences and confirmed experimentally. The numerical results of optimizing cell gap overcome the constraints of many approximations e.g. the small angle approximation and agree much better with the experimental data than those of analytical solution. Therefore, this method supplies a useful tool to achieve the optimal cell gap of a nematic LCWFC with high precision. Together with high birefringence and low rotational viscosity liquid crystal (LC) material effect, a nematic LCWFC with response time of sub-millisecond can be achieved in the visible spectral region.

1. Introduction

In recent years, technological progress especially the development of wavefront corrector has enabled liquid–crystal adaptive optics systems (LCAOSs) to be widely applied to large-aperture telescopes [1–3]. There are two major wavefront correctors: deformable mirrors (DMs) and nematic liquid–crystal wavefront correctors (LCWFCs). The response speed of DMs is enough fast, but the finite number of actuators of DMs cannot meet the demand of telescopes with apertures of tens of meters [3,4]. LCWFCs have the advantages of large number of correcting elements, high reliability, low power consumption, compactness, low cost and possibility of batch production [5–7]. However, the main shortcoming of a slow response time makes it difficult to meet the demand of telescopes with apertures of tens or even hundreds of meters [3,8,9]. To improve the response speed of the LCWFC, many materials have been considered [10–13], especially dual frequency and ferroelectric LC materials [14,15]. However, due to its high operating voltage requirement and the complexity of the control method, the dual frequency LCWFC has difficulty in handling millions of active elements. The binary phase modulation of ferroelectric LCs limits their effectiveness in WFCs. Compared with dual frequency and ferroelectric LC materials, nematic LC should be a nice choice. Gauza et al. have achieved some new nematic LC materials with a high response speed [16–18]. So in this paper, only nematic LC materials will be utilized to obtain fast response LCWFC.

For nematic LCWFCs, kinoform technique is widely used in order to expand the phase modulation to several, even tens of microns [19]. This technique, however, requires at least 2π phase modulation for transmissive LCWFCs (at least π for reflective LCWFCs). Therefore, it is very important to enhance the response speed of LCWFCs at a specific modulation quantity. For nematic LC materials, in order to achieve a fast response time, high birefringence (Δn) and low rotational viscosity (γ_1) LC mixtures, also called high figure-of-merit (FoM$=K_{11}\Delta n^2/\gamma_1$) mixtures, are preferred [20,21]. Another straightforward approach is to use a thin cell, since normally both rise time and decay time are known to be proportional to d^2 [22,23]. Shin-Tson Wu et al. pointed out that in the large signal regime the optical decay time is independent of the cell gap [23,24]. Wang et al. discussed the physical picture of the optical response time as a function of the cell gap in different voltage regions [22]. They emphasized that the theoretical derivation of this d^2 dependence is based on the small angle and $K_{11}\approx K_{33}$ approximations, and the optical response time in the middle voltage regime is linearly proportional to d. In addition, Peng et al. have recently analyzed the response time as a function of the cell gap at a specific phase retardation [9]. They indicated that the response time of 2π first decreases and then increases with the LC cell gap increasing, and there is an optimal cell gap to obtain the

* Corresponding author.
E-mail address: peng@ciomp.ac.cn (Z. Peng).

0030-4018/$ - see front matter © 2013 Elsevier B.V. All rights reserved.
http://dx.doi.org/10.1016/j.optcom.2013.05.028

shortest response time. From then on, it is novel and significant to improve the response time of LCWFC using optimal cell gap. However, it is a pity that their analytical solution of the optimal cell gap is based on many approximations, especially the small angle approximation and the initial average rotation angle approximation. We find that these approximations cannot hold well in practical applications. Furthermore, the calculations on optimal cell gaps of other optical modes e.g. OCB(Optically Compensated Bend) should take other factors into account e.g. shear-flow [25], so it is difficult to get the analytical solution and numerical calculation on optimal cell gap is necessary. In this paper, we derive the optimal cell gap of a nematic liquid–crystal wavefront corrector by a finite difference iterative method, and the confirming experimental results agree better with the theoretical derivation compared with the analytical solution. Based on the numerical method, the response time of some high FoM nematic mixtures in Refs. [17,18] at respective optimal cell gaps are given, which suggests that they have enormous fast response potentials to be drawn utilizing the optimal cell gap.

2. Theory

The main task for calculating optimal cell gap of a LCWFC is to calculate the deformation profile of a liquid-crystal director inside the cell under an applied voltage. Now several methods e.g. Newton method and relaxation method have been developed to calculate the director profile under a given applied voltage [26–28]. In this paper, we use a numerical method proposed by Wang et al. to calculate director deformation profile [29], which is based on finite-difference approximation to the Ericksen–Leslie equation. The configuration as a prototype of a LCWFC is shown in Fig. 1, d is the cell gap, θ is the tilt angle measured from the surface toward director and there is no consideration of the twist angle. Furthermore, in the strong anchoring case the pretilt angles θ_1 and θ_{N-1} are fixed on the cell surfaces. In our calculation, the cell is divided into 100 layers, i.e. $N=101$.

When the backflow and inertial effects are ignored, the dynamics of the LC director reorientation is described by the following Ericksen–Leslie equation [30–32]:

$$\gamma_1\frac{\partial\theta}{\partial t}=(K_{11}\cos^2\theta+K_{33}\sin^2\theta)\frac{\partial^2\theta}{\partial z^2}+(K_{33}-K_{11})\sin\theta\cos\theta\left(\frac{\partial\theta}{\partial z}\right)^2+\varepsilon_0\Delta\varepsilon\left(\frac{\partial U}{\partial z}\right)^2\sin\theta\cos\theta \tag{1}$$

where γ_1 is the rotational viscosity, K_{11} and K_{33} are the elastic constants associated with splay and bend deformation, respectively, $\Delta\varepsilon$ is the LC dielectric anisotropy, $\partial U/\partial z$ is the electric field

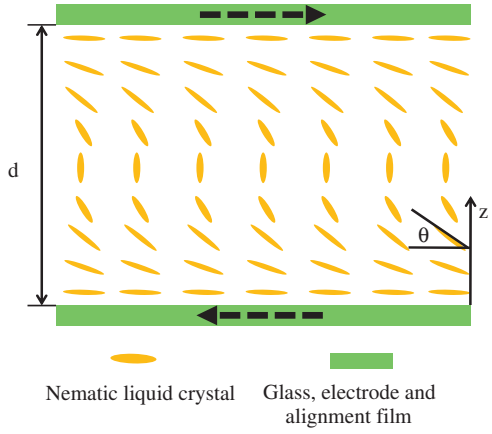

Fig. 1. Schematics of the parallel-aligned LC cell structure.

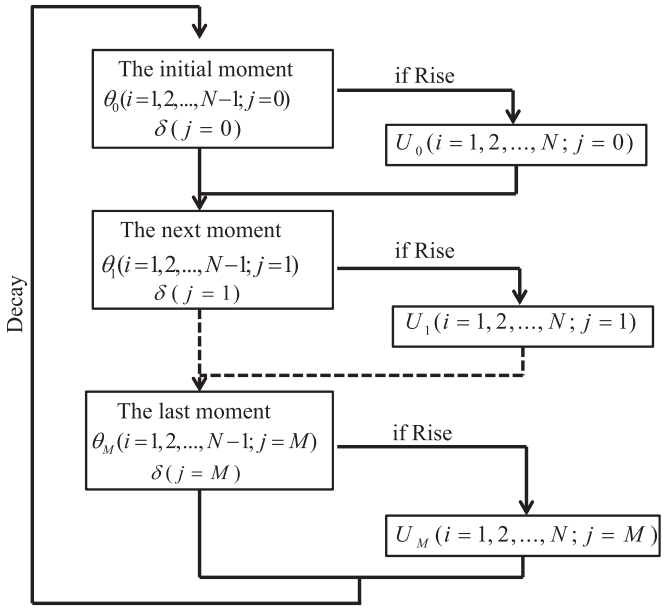

Fig. 2. The schematic diagram of the iterative computation including the tilt angle and voltage.

strength, which is governed by

$$(\varepsilon_\parallel\sin^2\theta+\varepsilon_\perp\cos^2\theta)\frac{\partial^2U}{\partial z^2}+2\frac{\partial U}{\partial z}\Delta\varepsilon\sin\theta\cos\theta\frac{\partial\theta}{\partial z}=0 \tag{2}$$

To obtain a numerical algorithm, we discretize $\partial^2\theta/\partial z^2$, $\partial\theta/\partial z$, $\partial U/\partial z$, $\partial^2U/\partial z^2$ and $\partial\theta/\partial t$ by central and forward finite differences, respectively.

$$\frac{\partial^2\theta}{\partial z^2}=\frac{\theta_{i+1,j}-2\theta_{i,j}+\theta_{i-1,j}}{(\Delta z)^2} \tag{3}$$

$$\frac{\partial\theta}{\partial z}=\frac{\theta_{i+1,j}-\theta_{i-1,j}}{2\Delta z} \tag{4}$$

$$\frac{\partial U}{\partial z}=\frac{U_{i+1,j}-U_{i-1,j}}{2\Delta z} \tag{5}$$

$$\frac{\partial^2U}{\partial z^2}=\frac{U_{i+1,j}-2U_{i,j}+U_{i-1,j}}{(\Delta z)^2} \tag{6}$$

$$\frac{\partial\theta}{\partial t}=\frac{\theta_{i,j+1}-\theta_{i,j}}{\Delta t} \tag{7}$$

Substituting these equations into Eqs. (1) and (2)

$$\theta_{i,j+1}=\theta_{i,j}+\frac{\Delta t}{\gamma_1}\left[(K_{11}\cos^2\theta_{i,j}+K_{33}\sin^2\theta_{i,j})\frac{\theta_{i+1,j}-2\theta_{i,j}+\theta_{i-1,j}}{(\Delta z)^2}+(K_{33}-K_{11})\sin\theta_{i,j}\cos\theta_{i,j}\left(\frac{\theta_{i+1,j}-\theta_{i-1,j}}{2\Delta z}\right)^2+\varepsilon_0\Delta\varepsilon\left(\frac{U_{i+1,j}-U_{i-1,j}}{2\Delta z}\right)^2\sin\theta_{i,j}\cos\theta_{i,j}\right] \tag{8}$$

$$(\varepsilon_\parallel\sin^2\theta_{i,j}+\varepsilon_\perp\cos^2\theta_{i,j})\frac{U_{i+1,j}-2U_{i,j}+U_{i-1,j}}{(\Delta z)^2}+2\frac{U_{i+1,j}-U_{i-1,j}}{2\Delta z}\Delta\varepsilon\sin\theta_{i,j}\cos\theta_{i,j}\frac{\theta_{i+1,j}-\theta_{i-1,j}}{2\Delta z}=0 \tag{9}$$

where $\theta_{i,j}$ and $U_{i,j}$ denote the tilt angle and voltage of the ith layer and the jth moment, respectively. $\theta_{i,j+1}$ denotes the tilt angle of the next moment. In order to get the director profile at any time, we must calculate the director profile and voltage profile simultaneously. If the tilt angle θ and voltage U at the initial moment are

given, the director profile and voltage profile at any time can be known according to Eqs. (8) and (9).

Since the rise time is much shorter than the decay time which is primarily governed by the free relaxation of the elastic distortion torque, we only focus on the decay time. For the turn-off process, the LC cell is initially biased at a high voltage and we can get the whole director profile by Eqs. (8) and (9) which is taken as the initial state. Then the voltage is removed instantaneously at $t=0$, the time-dependent phase change associated with this angle change is described as follows:

$$\delta = \frac{2\pi}{\lambda}\int_0^d \left[\frac{n_e n_o}{(n_e^2\sin^2\theta + n_o^2\cos^2\theta)} - n_o\right] dz \tag{10}$$

Using finite differences, the integral should be replaced by a sum of discrete phase changes. Thus, Eq. (10) is rewritten as:

$$\delta(j) = \frac{2\pi}{\lambda}\sum_{i=1}^{100}\left[\frac{n_e n_o}{(n_e^2\sin^2\theta_{i,j} + n_o^2\cos^2\theta_{i,j})} - n_o\right]\Delta z \tag{11}$$

where n_e and n_o are the refractive indices for the extraordinary and ordinary rays, respectively, λ is the wavelength. The whole schematic diagram of the iterative computation can be expressed as follows:

3. Experiment and results

To validate Ericksen–Leslie equation and numerical calculation results, the electro-optic measurement of a homogeneous cell with cell gap $d=7.98$ μm at $T=25$ °C is carried out. The cell is coated with indium–tin–oxide (ITO) electrodes, and on the top of ITO, the substrate is covered with a thin polyimide alignment film. The buffing induced pretilt angle is about 4° which is measured by LCD device parameters comprehensive test instrument (LCT-5016 series). A laser ($\lambda=730$ nm) is used as the light source. The linear polarizer is orientated at 45° with respect to the LC rubbing direction and the analyzer is crossed. The light transmittance is measured by a photodiode detector (New Focus Model 2031) and displayed by a digital oscilloscope (Tektronix MSO 3032). A common commercial nematic LC 5CB (pentylcyanobiphenol) is used in our experiments and numerical calculations. The material parameters of 5CB [33–36] are, refractive indices $n_e=1.698$ and $n_o=1.526$, the elastic constants $K_{11}=6.0\times10^{-12}$ N and $K_{33}=8.4\times10^{-12}$ N, the dielectric anisotropy $\Delta\varepsilon=11.5$, the rotational viscosity $\gamma_1=64$ mPa s. An ac (alternating current) 9.09 V voltage with 1 kHz square waves was used to drive the LC cell and it was removed at $t=0$.The experimental and simulated transient phase changes are depicted in Fig. 3. Here we consider the case of transmissive LCWFC first, i.e. the response time is obtained at the phase retardation of 2π.

It is clear that the calculation data match the experimental results quite well except the first few milliseconds, which means that Ericksen–Leslie equation regardless of backflow and inertial effects is feasible to calculate the director deformation profile, what is more, the method of numerical calculation is reliable to calculate the transient phase change and optimal cell gap of a LCWFC. The response time from the beginning to the instant of 2π phase is plotted in Fig. 3.

The complete physical picture of response time of 2π as a function of cell gap is shown in Fig. 4. The numerical results are obtained according to those equations above, while the concrete analytical method of the response time is detailed in Ref.[9]. On the one hand, as shown in Fig. 4, the trends of all of phase changes as a function of cell gap are consistent, which means that the

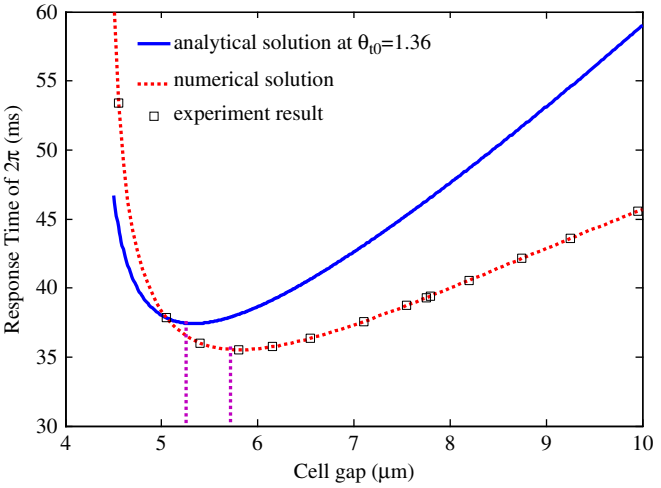

Fig. 4. Measured and calculated response time of 2π as a function of the cell gap, where the empty squares show the experimental results, the blue line and the red dot line correspond to the results derived from analytical solution and numerical solution. (For interpretation of the references to color in this figure legend, the reader is referred to the web version of this article.)

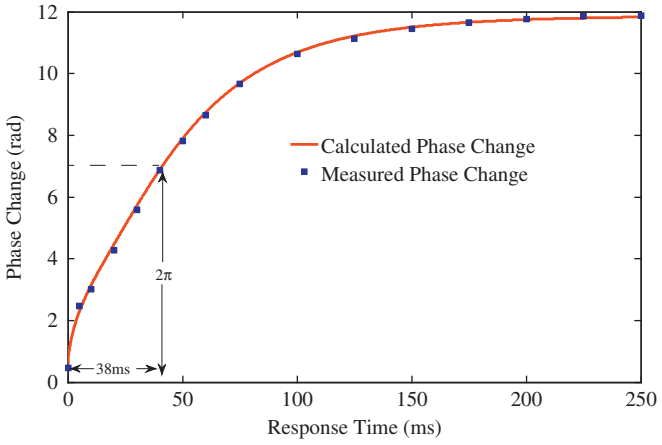

Fig. 3. The experimental and calculated transient phase changes of a 7.98 μm homogeneous 5CB cell with 4° pretilt angle at $T=25$ °C and $\lambda=730$ nm released from $V_i=9.09$ V_{rms}. The red line shows the calculated transient phase change, while the filled squares are the experimental data. (For interpretation of the references to color in this figure legend, the reader is referred to the web version of this article.)

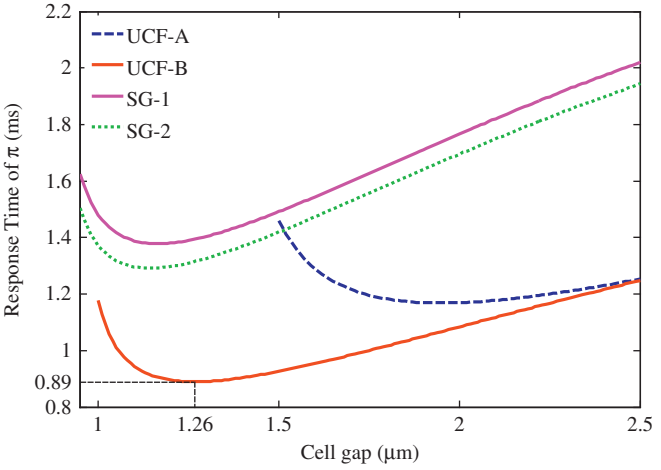

Fig. 5. The response time of four different high figure-of-merit (FOM) nematic mixtures as a function of cell gap: UCF-A (blue dash line), UCF-B (red line), SG-1 (magenta line) and SG-2 (green dot line). (For interpretation of the references to color in this figure legend, the reader is referred to the web version of this article.)

Table 1
The physical properties and response performances of four different high FoM nematic mixtures. d_{opt} represents the optimal cell gap, T_{opt} is the response time of π at the optimal cell gap, $T_{2.5}$ is the response time of π at the cell gap of 2.5 μm.

Mixture	K_{11} (pN)	K_{33} (pN)	$\varepsilon_{\parallel}$	$\varepsilon_{\perp}$	Δn	γ_1 (mPa•s)	FoM ($\mu m^2 s^{-1}$)	d_{opt} (μm)	T_{opt} (ms)	$T_{2.5}$ (ms)	$(T_{2.5}-T_{opt})/T_{2.5}$ (%)
UCF-A	15.6	54.9	13.5	3.0	0.254	99.84	10.1	1.95	1.1684	1.2530	6.75
UCF-B	20.9	40.2	19.9	4.2	0.354	140	18.7	1.27	0.89	1.2475	28.66
SG-1	15.8	9.8	21.2	4.6	0.38	189.6	12.0	1.16	1.3782	2.02	31.77
SG-2	20.7	31.8	19.8	4.2	0.38	207	14.4	1.14	1.2915	1.9437	33.55

response time of 2π first decreases and then increases with the LC cell gap increasing and the optimal cell gap really does exist. On the other hand, it is obvious that the data of numerical calculation agree with the experiment quite well in the whole regime, however, the analytical solution is unsatisfactory by reason of the assumed average rotation angle θ_{to} and so forth. In other words, the numerical method is more accurate to get the optimal cell gap of a LCWFC.

Fig. 5 depicts the response time of four different high FoM nematic mixtures proposed by Gauza et al. [17,18], their physical properties and response performances are listed in Table 1. Here, the reflective LCWFC is considered which is widely used in practical applications, so the response time is obtained at the phase retardation of π. Firstly, from Table 1, only with optimal cell gap effect and LC material effect, reflective LCWFC with response time of sub-millisecond can be achieved, especially the response time of UCF-B at $d_{opt}=1.27$ μm and $\lambda=633$ nm can be 0.89 ms. What is more, together with over-driven technique and optimal temperature effect, the response time of LCWFC can be further improved. Subsequently, Table 1 lists the response time of π at the cell gap of 2.5 μm as a specific example, i.e. $T_{2.5}$. Compared with $T_{2.5}$, T_{opt} increases by around 30%, which means that the optimal cell gap effect can increase the response speed of up to 30% in this situation. Finally, from Table 1, in general, the FoM is consistent with T_{opt}, but there are some exceptions. It appears that T_{opt} can give us a more intuitive understanding of response performance of LC material.

4. Conclusion

To summarize, we have further analyzed theoretically and confirmed experimentally the optimal cell gap of a LCWFC. This paper gives the complete process for obtaining the optimal cell gap. The numerical method based on finite differences has been proved to be more accurate and reliable to get the optimal cell gap. This approach will be helpful to achieve the shortest response time at specific phase retardation in wavefront correctors and we have proved to get the reflective LCWFC with response time of 0.89 ms only utilizing the optimal cell gap effect and LC material effect. These results indicate that with the development of new techniques and new LC materials, a nematic LCWFC with response time on a par with deformable mirrors can be achievable.

Acknowledgment

This work was supported by the National Science Foundation of China (11174274, 11174279, 61205021 and 11204299) and the Science Foundation of State Key Laboratory of Applied Optics.

References

[1] S.P. Kotova, M.Y. Kvashnin, M.A. Rakhmatulin, O.A. Zayakin, I.R. Guralnik, N. A. Klimov, P. Clark, G.D. Love, A.F. Naumov, C.D. Saunter, M.Y. Loktev, G. V. Vdovin, L.V. Toporkova, Optics Express 10 (2002) 1258.
[2] Z.L. Cao, Q.Q. Mu, L.F. Hu, X.H. Lu, L. Xuan, Optics Express 17 (2009) 17715.
[3] Z.L. Cao, Q.Q. Mu, L.F. Hu, Y.G. Liu, L. Xuan, Optics Communications 283 (2010) 946.
[4] D.J. Hoppe, IPN Progress Report, 42–147 (2001) 1–14.
[5] D.M. Cai, N. Ling, W.H. Jiang, Proceedings of SPIE 6457 (2007) 64570P.
[6] X.H. Wang, B. Wang, J. Pouch, F. Miranda, J.E. Anderson, P.J. Bos, Optical Engineering 43 (2004) 2769.
[7] H.X. Zhang, J. Zhang, L.Y. Wu, Measurement Science and Technology 18 (2007) 1724.
[8] L.F. Hu, L. Xuan, Y.J. Liu, Z.L. Cao, D.Y. Li, Q.Q. Mu, Optics Express 12 (2004) 6403.
[9] Z.H. Peng, Y.G. Liu, L.S. Yao, Z.L. Cao, Q.Q. Mu, L.F. Hu, L. Xuan, Optics Letters 36 (2011) 3608.
[10] I. Dierking, Advanced Materials 12 (2000) 167.
[11] H. Kikuchi, M. Yokota, Y. Hisakado, H. Yang, T. Kajiyama, Nature Materials 1 (2002) 64.
[12] Y.H. Fan, Y.H. Lin, H.W. Ren, S. Gauza, S.T. Wu, Applied Physics Letters 84 (2004) 1233.
[13] H.W. Ren, Y.H. Lin, S.T. Wu, Applied Physics Letters 88 (2006) 061123.
[14] D.C. Burns, I. Underwood, J. Gourlay, A. Ohara, D.G. Vass, Optics Communications 119 (1995) 623.
[15] S.R. Restaino, D. Dayton, S. Browne, J. Gonglewski, J. Baker, S. Rogers, S. McDermott, J. Gallegos, M. Shilko, Optics Express 6 (2000) 2.
[16] S. Gauza, H.Y. Wang, C.H. Wen, S.T. Wu, A.J. Seed, R. Dabrowski, Japanese Journal of Applied Physics 42 (Part 1) (2003) 3463.
[17] S. Gauza, J. Li, S.T. Wu, A. Spadlo, R. Dabrowski, Y.N. Tzeng, K.L. Cheng, Liquid Crystal 32 (2005) 1077.
[18] S. Gauza, C.H. Wen, B. Wu, S.T. Wu, A. Spadlo, R. Dabrowski, Liquid Crystal 33 (2006) 705.
[19] Z.L. Cao, L. Xuan, L.F. Hu, Y.J. Liu, Q.Q. Mu, Optics Express 13 (2005) 5186.
[20] Y. Goto, T. Ogawa, S. Sawada, S. Sugimori, Molecular Crystals and Liquid Crystals 209 (1991) 1.
[21] P.F. McManamon, T.A. Dorschner, D.L. Corkum, L.J. Friedman, D.S. Hobbs, M. Holz, S. Liberman, H.Q. Nguyen, D.P. Resler, R.C. Sharp, E.A. Watson, Proceedings of the IEEE 84 (1996) 268.
[22] H.Y. Wang, X.Y. Nie, T.X. Wu, S.T. Wu, Molecular Crystals and Liquid Crystals 454 (2006) 285.
[23] S.T. Wu, C.S. Wu, Applied Physics Letters 53 (1988) 1794.
[24] A.E. Perregaux, U.S.Patent, No.4,595,259 (1986).
[25] H.F. Cheng, H.J. Gao, Liquid Crystals 28 (2001) 1337.
[26] C.J. Chen, A. Lien, M.I. Nathan, Journal of Applied Physics 81 (1997) 70.
[27] D.W. Berreman, Applied Physics Letters 25 (1974) 12.
[28] C.Z. Vandoorn, Journal of Applied Physics 46 (1975) 3738.
[29] Q. Wang, S.L. He, F.H. Yu, N.R. Huang, Optical Engineering 40 (2001) 2552.
[30] J.L. Ericksen, Transactions of the Society of Rheology 5 (1961) 23.
[31] F.M. Leslie, Archive for Rational Mechanics and Analysis 28 (1968) 265.
[32] F.M. Leslie, Continuum Mechics and Thermodynamics 4 (1992) 167.
[33] S.T. Wu, C.S. Wu, M. Warenghem, M. Ismaili, Optical Engineering 32 (1993) 1775.
[34] R.D. Polak, G.P. Crawford, B.C. Kostival, J.W. Doane, S. Zumer, Physical Review E 49 (1994) R978.
[35] P.G. Cummins, D.A. Dunmur, D.A. Laidler, Molecular Crystals and Liquid Crystals 30 (1975) 109.
[36] R.P. Pan, S.M. Chen, T.C. Hsieh, Molecular Crystals and Liquid Crystals 198 (1991) 99.